Dynamics of optically induced nuclear spin polarization in individual InP/$Ga_xIn_{1-x}P$ quantum dots

E. A. Chekhovich,[1,2] M. N. Makhonin,[1] J. Skiba-Szymanska,[1,*] A. B. Krysa,[3] V. D. Kulakovskii,[2] M. S. Skolnick,[1] and A. I. Tartakovskii[1]

[1]*Department of Physics and Astronomy, University of Sheffield, Sheffield S3 7RH, United Kingdom*

[2]*Institute of Solid State Physics, Chernogolovka 142432, Russia*

[3]*Department of Electronic and Electrical Engineering, University of Sheffield, Sheffield S1 3JD, United Kingdom*

(Received 28 December 2009; revised manuscript received 16 March 2010; published 9 June 2010)

We report on dynamics of optically induced nuclear spin polarization in individual InP/GaInP quantum dots at $T=4.2$ K. Dots with different charge states arising from residual doping in a nominally undoped sample have been studied. In the same sample, we find strong dot-to-dot variation in the nuclear spin decay times in the dark from ~85 to ~6000 s. The longest decay times measured are comparable to those previously measured in bulk InP and correspond to almost complete suppression of nuclear spin diffusion out of the dot. In the negatively charged dots, the spin decay times exceed 300 s (with the slowest decay of ~6000 s), about 10^5 times longer than those reported previously in electron charged dots in gated structures. We discuss possible mechanisms responsible for suppression of nuclear spin diffusion, including inhomogeneous quadrupolar shifts and stabilizing effect of the hyperfine interaction with the electron confined in the dot.

DOI: 10.1103/PhysRevB.81.245308 PACS number(s): 73.21.La, 75.75.−c, 78.55.Cr

I. INTRODUCTION

Recent years have seen a strong rise in research on phenomena related to individual spins in different branches of solid-state physics. Such growth has largely been driven by developments in quantum information processing (QIP), for which individual spins have been predicted to form qubits with favorable properties.[1] These developments have also been supported by the fast progress in nanotechnology, which now enables access to individual spin states in various solid-state nanosystems and their control by optical and electrical means.

An essential requirement for a spin qubit will be long-lived spin memory and coherence relying on its effective isolation from the magnetic environment. In this respect, good candidates for solid-state implementation of QIP are materials with well-isolated nuclear spins such as ^{29}Si nuclei[2,3] and ^{31}P impurities[4,5] in silicon, nitrogen nuclei in $N@C_{60}$ molecules,[6] and ^{13}C (Refs. 7–9) in diamond.

In III-V semiconductors, favored for fabrication of advanced quantum dot (QD) nanostructures suitable for both electrical and optical control of single electron and hole spin states, all atoms carry nonzero nuclear spin. This results in efficient dissipation of information encoded in the spin degree of freedom due to spin nonconserving nuclear dipole-dipole interactions, introducing an uncontrollable dephasing in QD-based qubits.[10,11] Dynamic nuclear spin polarization enabling control over the magnetic environment is a possible way to circumvent this problem.[12–18] This approach will rely on the knowledge of the dynamic properties of the nuclear field in a nanostructure, in particular, the speed with which it is possible to change it by optical or electrical means, and also the persistence of the nuclear polarization once the spin pumping has been switched off.

Here we study the dynamic properties of nuclear spin polarization in InP/GaInP quantum dots with different charge states. In contrast to majority of previous studies of nuclear spin polarization in quantum dots, the charging in the studied dots arises from random residual doping in a nominally undoped semiconductor sample. The dynamics are studied at a low temperature of 4.2 K in a wide range of magnetic fields. Under nonresonant optical excitation, the fastest nuclear spin buildup time as short as ≈5 ms is found at zero magnetic field. Slower nuclear spin buildup dynamics characterized with rise times of ≈2 s are observed for $B \geq 2$ T. Nuclear spin depolarization in the absence of the optical pumping slows down when magnetic field is applied. In the dots studied, the decay times in the dark condition in a wide range of magnetic fields exceed by up to 10^3 the corresponding polarization buildup times under optical excitation. However, we also observe strong dot-to-dot variation in the decay time from ~85 to ~6000 s in the same sample, with the longest time comparable to decay time in bulk InP [≈7000 s (Ref. 19)] corresponding to nearly complete suppression of spin diffusion. Long spin lifetimes up to 6000 s are observed in electron-charged dots, in stark contrast to previous studies on Schottky structures where decay in electron-charged dots occurred on a millisecond time scale[20] while nuclear spin lifetime in an empty dot has been shown to exceed 1 h.[21]

We consider two possible sources of nuclear spin diffusion suppression responsible for long spin lifetimes: quadrupolar interaction (QI) and inhomogeneous effective magnetic field of the electron (Knight field). Inhomogeneous quadrupolar shifts of nuclear spin levels induced by elastic stress[22] were used recently to explain long nuclear spin lifetimes in InGaAs QDs.[21] In the studied InP/GaInP structures QI plays a significant role. We show, however, that understanding of spin dynamics in different dots requires consideration of additional relaxation mechanisms dependent on charge, structural properties, or the surrounding of each particular dot. An alternative model, studied theoretically recently,[23] relies on stabilizing influence of the inhomogeneous Knight field of the electron localized on the dot. In our case, the confined electron is uncoupled from the environment due to the ab-

 ©2010 The American Physical Society

sence of electric contacts. We show that this can lead to a closed electron-nuclear spin system with frozen nuclear dipole-dipole interaction and hence, suppressed diffusion. Random noise in the depolarization dynamics observed in a few cases in our measurements can be explained by dot recharging in the absence of photoexcitation. Such recharging can also explain the observed behavior in one singly positively charged dot where a long decay time exceeding 1 h has been measured.

The rest of the paper is organized as follows. In Sec. II we give a description of the studied structures and experimental technique. Section III gives experimental results on optical nuclear spin pumping in quantum dots with different charge states in a wide range of experimental conditions. Section IV is devoted to experimental studies of nuclear spin dynamics: in Sec. IV A dynamics of nuclear spin polarization under optical excitation (buildup dynamics) are considered while Sec. IV B presents results on spin decay dynamics in the dark. In Sec. V we discuss mechanisms of nuclear spin relaxation relevant to our experimental results. Finally, in the Appendix we give details of photoluminescence (PL) characterization of the studied dots.

II. SAMPLES AND EXPERIMENT

The samples with InP/GaInP QDs were grown by low-pressure metal organic vapor phase epitaxy on (100) GaAs substrates misoriented toward $\langle 111 \rangle$, in order to suppress the CuPt-type ordering in the GaInP matrix. The growth temperature (growth rate) was 690 °C (0.7 nm/s) and 650 °C (0.35 nm/s) for GaAs, GaInP layers and for InP QD layer, respectively. More detailed information can be found in Ref. 24, where a design of a sample grown on a substrate with 10° misorientation is given. We find that the structure grown using the same procedure but on a substrate with 3° misorientation has much lower quantum dot density compared to a 10° misoriented sample. This may be a result of increased density of monoatomic layer steps, acting as nucleation sites for quantum dot formation, in a sample with larger substrate misorientation.[25] In this work we use both 10° misoriented high-density (HD) and 3° misoriented low-density (LD) samples covered with metal shadow masks with 400–800 nm clear apertures that allow single quantum dots to be addressed optically.

A typical low-temperature PL spectrum of ensemble of InP/GaInP dots has a bimodal distribution with two broad peaks centered around 1.67 and 1.8 eV.[24] It has been shown that the low-energy band corresponds to emission from large fully developed dots that can accumulate large number of charges while high-energy distribution corresponds to luminescence of small disk-shaped partially developed dots.[26,27] In the present work we use the dots of the second type[24,28] whose emission consists of narrow lines at ~1.78–1.84 eV with spectral full width at half maximum ~60 μeV limited by spectrometer resolution. Experiments were performed on individual dots at a temperature of 4.2 K, in external magnetic field up to 8 T parallel or perpendicular to the sample growth axis Oz. The sample was excited with a laser at 1.88 eV, below the GaInP band gap.[26,29] The ground-state QD PL was collected and dispersed by a double 1 m spectrometer coupled with a charge coupled device (CCD).

The samples were not doped intentionally and did not have Schottky diode structures. As a result the charge state of the dots could not be controlled by external bias. However, due to the presence of impurities, combined with the effect of photodepletion[30] induced by laser excitation, quantum dots with different charging could be found in these structures. Using magnetospectroscopy and Hanle effect measurements we distinguish between PL lines corresponding to neutral excitons and trions from positively and negatively charged dots. In this work we use only those dots where PL spectrum is dominated by emission corresponding to only one charge state in a wide range of photoexcitation power. However, it cannot be excluded that in the absence of photoexcitation QD can change its charge state. Such recharging cannot be detected by means of PL spectroscopy but may have a significant effect on nuclear spin decay dynamics when the sample is held in the dark (see discussion in Sec. V). The details of sample characterization are given in the Appendix. These experiments also allow to determine magnetic properties of the charge carriers important in nuclear spin measurements: electron and hole g factors were found to be $g_{e,z} \approx +1.5$ and $g_{h,z} \approx +2.7$, respectively.

III. OVERHAUSER EFFECT IN InP/GaInP QUANTUM DOTS WITH DIFFERENT CHARGE STATES

The dynamic nuclear polarization occurs under circularly polarized optical excitation of the dot leading, initially, to pumping of the electron spin.[31] The hyperfine interaction leads to spin flip-flops between the electron and a single nucleus.[14,15,28,32,33] Macroscopic nuclear spin, accumulated on the dot as a result of the dynamic nuclear polarization, acts back on either the confined or photoexcited electron with an effective magnetic field B_N.[31,32] This results in the modification (Overhauser shift) of the electron energy spectrum manifested in the splitting $\Delta E = \mu_B[g_h B_z - g_e(B_z + B_N)]$ observed in the electron-hole recombination spectrum[34] [$g_{e(h)}$ is the electron (hole) g factor and μ_B electron Bohr magneton]. The maximum variation in ΔE corresponding to fully polarized nuclear spins is ≈230 μeV in InP.[35] The sign of B_N depends on the helicity of the circularly polarized excitation. In this work we measure ΔE to determine B_N, directly reflecting the degree of the nuclear spin polarization on the dot.

The efficiency of nuclear spin pumping strongly depends on the charge state of the dot, external magnetic field, and intensity of the circularly polarized laser.[15,17,24,36,37] Figure 1(a) shows normalized PL intensity of trions in negatively (X^-) and positively (X^+) charged dots (N1 and N2, respectively) and of exciton and biexciton in a neutral dot (N3) measured as a function of the laser pump power P_{exc}. For all quantum dots ground-state luminescence intensity reaches its maximum at $P_{exc}^{sat} \approx 25$ μW indicating maximum occupancy of the dot with a single photoexcited electron-hole pair. At higher excitation densities QD emission disappears in broad background luminescence that can arise from highly excited QD transitions or from delocalized electron-hole pairs in the

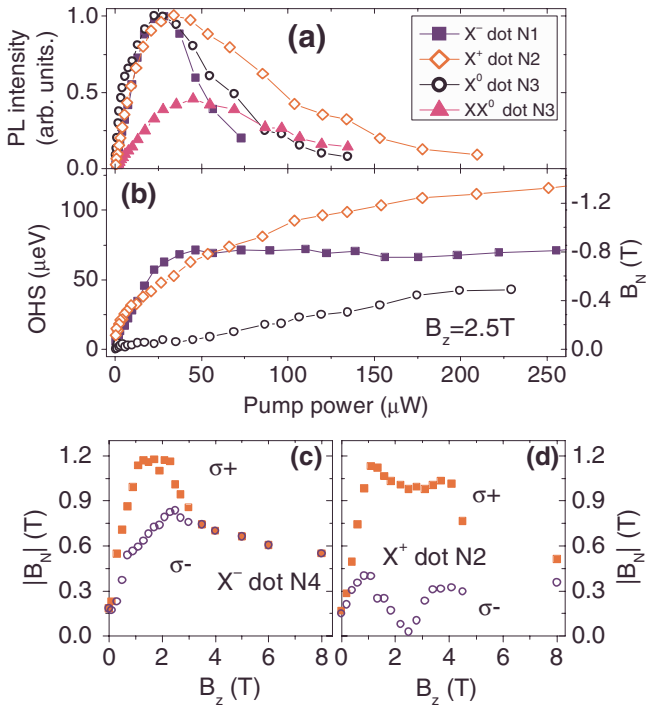

FIG. 1. (Color online) Results of the optical spin pumping experiments on quantum dots with different charging. (a) Normalized PL intensity as a function of pump power of the trion transitions in negatively (X^-) charged dot (N1), positively (X^+) charged dot (N2), and exciton (X^0) and biexciton (XX^0) transitions in a neutral dot (N3). (b) Overhauser splitting (OHS) and corresponding nuclear field as a function of the power of σ^+ excitation at B_z=2.5 T for the dots shown on panel (a). [(c) and (d)] Nuclear polarization $|B_N|$ as a function of magnetic field B_z under σ^+- (squares) and σ^-- (circles) polarized excitation at P_{exc}=70 μW in (c) negatively and (d) positively charged dots N4 and N2, respectively. In both cases $B_N<0$ ($B_N>0$) when excited with σ^+ (σ^-)-polarized laser.

wetting layer. Overhauser splitting (OHS) and corresponding nuclear field B_N are shown in Fig. 1(b) as a function of the pump power under σ^+-polarized excitation at B_z=2.5 T for the same dots as in Fig. 1(a). In order to measure the spectral splitting at high excitation density, when QD luminescence is suppressed, we use pump-probe techniques. A cycle consisting of a long, variable power pump pulse followed by a short low power probe is repeated periodically, with the PL measured only during the probe pulses. In order to reduce the effect of the probe on nuclear spin polarization in the dot, the pump and probe durations t_{pump} and t_{probe} are chosen to satisfy the condition $t_{pump} \gg \tau_{buildup} \gg t_{probe}$, where $\tau_{buildup}$ is the nuclear spin buildup time under optical pumping, measured in time-resolved experiments (see Sec. IV A).

In the charged quantum dots (both X^+ and X^-) steady-state nuclear spin polarization $|B_N|$ grows quickly with increasing excitation power P_{exc} and reaches ~0.6 T at P_{exc}^{sat} corresponding to the highest degree of QD occupancy with the exciton, observed as PL intensity maximum [Fig. 1(a)]. By contrast, comparable nuclear polarization in a neutral dot can only be achieved using high power excitation (P_{exc} >200 μW) resulting in almost complete suppression of QD PL. This suggests that nuclear spin polarization in negatively (positively) charged dots is induced by spin-polarized electrons (trions) localized on the dot[38] while in neutral dots nuclear polarization can build up due to the effect of delocalized carriers and can be accompanied by significant polarization in material surrounding the dot. Importantly for nuclear spin dynamics experiments, moderate power optical excitation of charged dots can be used to create considerable degree of nuclear polarization (up to ~50%) localized on the nanometer-scale volume of the dot only.

In the neutral quantum dots nuclear spin pumping is found to be ineffective at moderate optical power ($P_{exc} \approx P_{exc}^{sat}$) in a wide range of magnetic fields. In contrast to GaAs/AlGaAs dots,[33,39] in InP dots $|B_N|$ remains small even when magnetic field overcomes the effect of the fine-structure splitting at $B_z \gg \delta_b/(\mu_b|g_h - g_e|) \lesssim 1$ T, restoring electron-spin projections along Oz axis. We also find that in contrast to theoretical prediction,[40] no significant nuclear spin pumping takes place when energy splitting between J_z =+1 and J_z=+2 exciton levels with opposite electron spins is significantly reduced due to crossing of "dark" and "bright" exciton states at $B_z \approx 2.5$ T (see the Appendix). A complete description of the dynamic nuclear polarization process in dots with different charging requires detailed consideration of electron-hole capture/recombination dynamics as well as the hyperfine interaction in different exciton states of the dot, which is out of the scope of the present work. We note, however, that the low efficiency of nuclear spin pumping process in neutral dots is mainly due to the role of optically inactive (dark) exciton ground states, slowing down re-excitation of the dot. By contrast all spin states of the trion in both positively and negatively charged dots are optically allowed, enabling fast recycling of the spin-polarized electron.

In singly charged dots, excitation with circularly polarized light leads to $|B_N| \sim 0.2$ T even at zero magnetic field. Nuclear polarization $|B_N|$ as a function of external field B_z under σ^+ and σ^- excitations with a constant power P_{exc} =70 μW is shown for a negatively (positively) charged dot in Figs. 1(c) and 1(d). For both signs of QD charging nuclear field B_N is positive (negative) under σ^- (σ^+) excitation. Steady-state nuclear polarization is determined by the balance between the nuclear spin pumping rate w_s, controlled by optical excitation, and nuclear spin depolarization rate w_d. The latter also depends on optical excitation: relaxation of the nuclear spin during capture or recombination of the electron in the dot can be due to fluctuations of the electron Knight-field[33] or electric field gradients interacting with quadrupolar moments of In nuclei.[41] Stationary $|B_N|$ grows when magnetic field is increased from 0 to ~1 T due to suppression of nuclear spin depolarization. Nuclear spin pumping is especially effective under σ^+ excitation at B_z=1–3 T when optically induced nuclear field acts to reduce the electron Zeeman splitting and to enhance the electron-nuclear flip-flop rate. This positive feedback results in nuclear spin bistability and enhanced nuclear spin polarization.[17,24,42,43] Nuclear polarization under σ^- excitation is significantly smaller due to the negative feedback caused by $B_N>0$. In the positively charged dot X^+ N2 (LD-sample) nuclear polarization under σ^--polarized laser is almost completely suppressed at $B_z \approx 2.5$ T, observed as a dip in B_N in Fig. 1(d). This may be a combined effect of magnetic field dependence

of electron-to-nuclei spin transfer rate w_s, nuclear spin depolarization rate w_d, hole spin-relaxation rate, and the trion spin-polarization degree. At high B_z the Overhauser shift caused by B_N becomes small compared to the electron Zeeman splitting, thus reducing the strength of the feedback in the electron-nuclear system. As a result, the difference between σ^+- and σ^--polarized excitation becomes less pronounced as observed in Figs. 1(c) and 1(d).

IV. NUCLEAR SPIN DYNAMICS

A. Dynamics of nuclear spin polarization under optical pumping (nuclear spin buildup dynamics)

The electron-to-nuclei spin transfer rate

$$w_s \sim |A_{hf}|^2/(\Delta E_e^2 + \gamma^2/4), \tag{1}$$

where A_{hf} is the hyperfine interaction constant, γ is the electron-spin state broadening, and $\Delta E_e = \mu_B g_e (B_z + B_N)$ is the electron-spin splitting,[31] decreases significantly when $\Delta E_e \gg \gamma$ due to the energy conservation during the "flip-flop" process. Strong magnetic field dependence of w_s and the feedback in the electron-nuclear spin system result in a complicated nuclear spin dynamics in a charged QD.[44] Kinetics of nuclear spin polarization under optical pumping (referred to as nuclear spin buildup below) at various B_z has been studied experimentally using time resolved techniques. Temporal resolution was achieved by using either mechanical shutters with time accuracy ~ 2 ms at $B_z \neq 0$ or high-speed electro-optic and acousto-optic modulators at $B=0$. Time diagram of a single experiment cycle is shown in Fig. 2(a). First, long circularly polarized erase pulse initializes nuclear spins on the dot removing any polarization left from the previous cycle. Immediately after that, a pump pulse of variable duration, with the helicity opposite to that of the erase pulse, creates nuclear polarization of the opposite sign. The shutter of the detection system is opened after a t_{pump} delay from the beginning of the pump for a detection time t_{det}. This cycle is repeated several times to achieve good signal-to-noise ratio in the PL spectra, from where we deduce the trion (or exciton) spectral splitting and hence B_N.

The dependence of the spectral splitting on the pump time t_{pump} gives a transient curve of B_N, enabling measurements of the dynamics of nuclear spin buildup. In order to measure the dynamics for a wide range of t_{pump} the duration of the erase pulse t_{erase} and detection time t_{det} are also varied, according to the rule $t_{erase} = 8t_{pump}$ and $t_{det} = t_{pump}/4$. In this experiment we use pump and erase pulse of the same excitation power ≈ 70 μW. In the limit of long t_{pump}, the nuclear field reaches a steady-state value B_N, which depends on the external magnetic field, polarization, and power of excitation as shown in Figs. 1(c) and 1(d).

Nuclear spin buildup dynamics of B_N in a negatively charged dot X^- N4 are shown in Figs. 2(b) and 2(c) for $B_z = 0$ and 2 T (σ^+ pump) and 0.4 T (σ^+ and σ^- pumps). As expected from Eq. (1) external magnetic field significantly slows down nuclear spin buildup dynamics. At zero field B_N reaches its steady state during several milliseconds, whereas this requires several seconds at $B_z = 2$ T. Nonlinear dependence of w_s on B_N also results in nonexponential kinetics of nuclear polarization. This has a notable manifestation at small fields $B_z \approx 0.2$–0.6 T, where B_N can compensate B_z enhancing electron-nuclear spin transfer rate and nuclear spin bistability is observed.[24] The time dependence of B_N after switching polarization of excitation from $\sigma^{+(-)}$ to $\sigma^{-(+)}$ at $B_z = 0.4$ T shown with open (solid) triangles in Fig. 2(c) is strongly asymmetric with respect to the pump-laser helicity. For σ^--polarized pump the initial rise of B_N from nuclear polarization achieved during σ^+-polarized erase pulse ($B_N \approx -0.6$ T) to the polarization measured for shortest pump time ($B_N \approx -0.15$ T) is not time-resolved experimentally. This suggests that the buildup of B_N from -0.6 to -0.15 T, shown by the dashed arrow in Fig. 2(c), takes place during the shortest pump time $t_{pump} = 7$ ms determined by the resolution of the mechanical shutters. For the σ^--polarized pump a slow change in B_N is observed for $t_{pump} > 1$ s while for σ^+ pump B_N abruptly reaches a constant value after $t_{pump} \sim 0.2$ s. In the latter case the observed sharpness of transition is limited by averaging of the PL signal during the detection time $t_{det} = t_{pump}/4$. Thus the highest nuclear field variation rate $|dB_N/dt|$ is observed at $B_N \sim -B_z$, corresponding to the maximum of the electron-nuclear spin-flip rate w_s at $\Delta E_e \sim 0$ [see Eq. (1)].

As nuclear spin buildup is not exponential we use pump time $\tau_{buildup}$ required to reach a change in B_N equal to 70% of

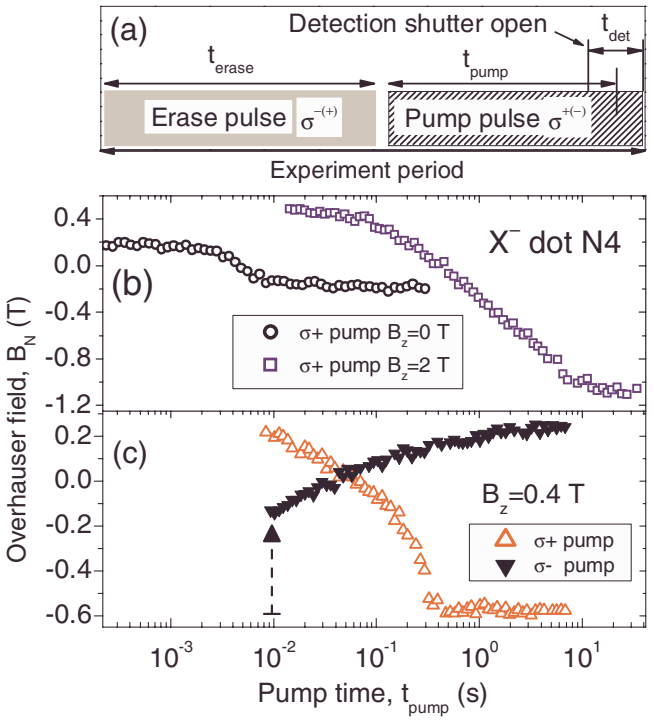

FIG. 2. (Color online) (a) Time diagram of the measurement of the nuclear polarization buildup dynamics in a single dot. In this experiment t_{pump} is varied as an independent variable while $t_{erase} = 8t_{pump}$, $t_{det} = t_{pump}/4$, and excitation power of both pulses is ≈ 70 μW. [(c) and (d)] Overhauser field B_N buildup dynamics in the negatively charged dot X^- N4 at $B_z = 0$ (circles), 0.4 T (triangles), and 2 T (squares). Open (solid) symbols correspond to σ^- erase/σ^+ pump (σ^+ erase/σ^- pump) experiments. Dashed arrow shows initial increase in B_N not resolved in the experiment.

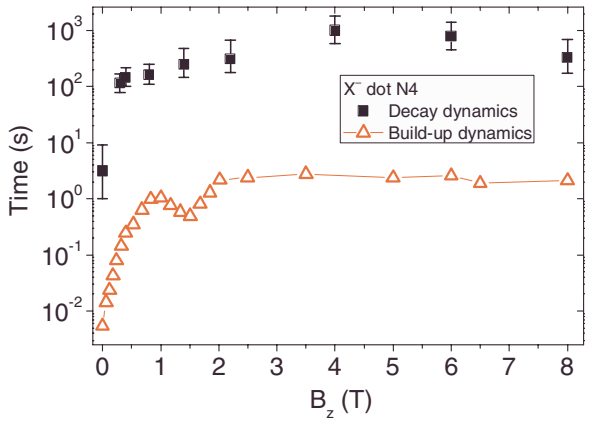

FIG. 3. (Color online) Magnetic field dependence of the nuclear spin buildup time under σ^+-polarized optical pumping (open symbols) and of the spin decay time in the dark condition (solid symbols) in a negatively charged dot X^- N4 (HD sample).

the temporal dynamic range $B_N(t_{pump}\to\infty)-B_N(t_{pump}\to 0)$ as a measure of the nuclear spin kinetics. The dependence of $\tau_{buildup}$ in the negatively charged dot N4 on B_z for σ^+-polarized pump is shown in Fig. 3 with triangles. The nuclear spin buildup time increases from $\tau_{buildup}\approx 5$ ms at $B=0$ to $\tau_{buildup}\approx 2.5$ s at $B_z=2$ T, which confirms the resonancelike dependence of the nuclear spin transfer rate on the electron-spin splitting. However, the simple rate equation model, proposed in Ref. 44 with spin transfer rate given by Eq. (1) does not describe quantitatively the observed nuclear spin dynamics in the whole range of B_z. In particular, it cannot also explain the saturation of $t_{buildup}$ at $B_z>2$ T. This discrepancy might be the evidence of several competing processes leading to the dynamic nuclear polarization.

We find that the nuclear spin buildup time in positively charged dots has the same strong dependence on the external field increasing from $\tau_{buildup}\approx 4$ ms at $B=0$ to $\tau_{buildup}\approx 2$ s at $B_z\geq 2$ T. In the neutral dot, where the nuclear spin pumping is only possible for high excitation power in external magnetic field (see Sec. III), the buildup time $\tau_{buildup}\approx 1$ s is found for pump power $P_{exc}=400$ μW at $B_z=4.1$ T.

B. Dynamics of nuclear spin polarization in the absence of optical excitation (nuclear spin decay dynamics)

Measurements of the nuclear spin lifetime in individual dots have been carried out with a pump-probe method based on the single-dot PL detection. The time diagram of the nuclear spin decay measurement is shown schematically in the inset of Fig. 4(b). The nuclear spin polarization B_N^{pump} is induced by a circularly polarized pump pulse with a duration t_{pump}. Photoexcitation is then blocked for a time t_{delay} by a mechanical shutter insuring complete suppression of the stray light. After a delay, the nuclear polarization is measured in PL excited with a short probe pulse t_{probe}. The durations of the pulses were chosen to be $t_{probe}\ll t_{buildup}\ll t_{pump}$ in order to ensure that the pump pulse initializes nuclear polarization to a certain level, and that B_N does not change significantly during the excitation with the probe. In our experiments these times were chosen to be $t_{pump}\approx 7\times t_{buildup}$ and $t_{probe}\approx t_{buildup}/10$. Due to the strong dependence of $t_{buildup}$ on B_z (see Sec. IV A), these conditions required shortening of t_{probe} in low magnetic fields and led, for example, to t_{probe} at $B_z\leq 0.3$ T shorter than the time needed for PL measurements with an acceptable signal-to-noise ratio. In those cases the cycle shown in the inset in Fig. 4 is repeated several times and B_N averaged over several cycles is measured. By contrast, at high B_z detection in a single probe pulse allows to measure the instantaneous value of B_N in a single quantum

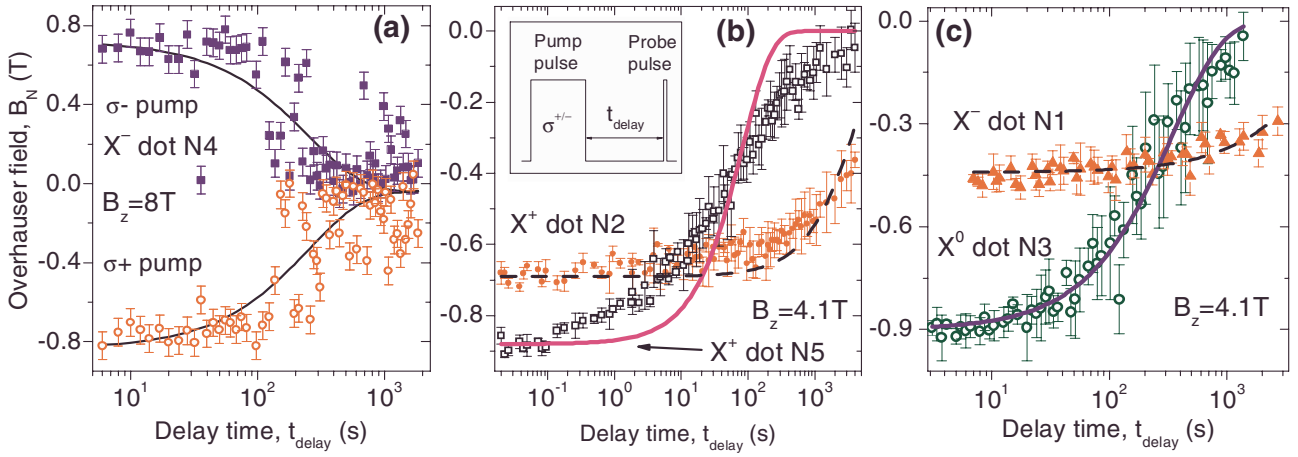

FIG. 4. (Color online) Nuclear spin decay dynamics. Inset shows a diagram of the cycle in the pump-probe experiment. The power of the pump has been chosen at a level corresponding to the maximum PL intensity $P_{exc}\sim P_{exc}^{sat}$ with an exception for the neutral dot X^0, where high power pump $P_{exc}\sim 15P_{exc}^{sat}$ has been used. (a) Decay of nuclear spin polarization in a negatively charged dot (X^- N4, HD sample) at $B_z=8$ T. Squares and circles show data measured with σ^-- and σ^+-polarized pumps, respectively. For delays $t_{delay}>100$ s large fluctuations of B_N in X^- N4 can be seen, demonstrating that nuclear spin decay is a random discrete process. Solid lines show an exponential function with $\tau_{dec}\approx 250$ s. (b) Nuclear spin decay in positively charged dots (X^+ N2 and N5, LD sample) at $B_z=4.1$ T. Exponential fit with $\tau_{dec}\approx 4200$ s (85 s) is shown with the dashed (solid) line for dot N2 (N5). (c) Nuclear spin relaxation in a negatively charged dot (X^- N1, LD sample) and in a neutral dot (X^0 N3, LD sample) at $B_z=4.1$ T. Exponential fit with $\tau_{dec}\approx 5800$ s (350 s) is shown with the dashed (solid) line for dot X^- N1 (X^0 N3).

dot. The necessity to repeat multiple cycles during the single accumulation at small B_z also limits the longest possible t_{delay} due to limited maximum exposure time of the CCD camera. As a result at zero field the maximum $t_{delay} \approx 15$ s can be employed while at high magnetic field the longest delay used $t_{delay} \approx 4000$ s is limited only by the total experiment time of ~40 h.

Excitation power of the pump pulse P_{exc} in the experiments on charged dots has been chosen at a relatively low level roughly corresponding to the maximum intensity of the ground-state trion PL $P_{exc} \approx P_{exc}^{sat}$ (see Sec. III). Under this condition, PL spectra consist mainly of the QD emission lines and thus the pump creates large nuclear polarization localized in a nanometer-scale volume of the dot. Small efficiency of the optical spin pumping in neutral dots requires the use of high power excitation $P_{exc} \approx 15 P_{exc}^{sat}$ in order to create measurable B_N. At this P_{exc} the ground-state QD PL is suppressed and strong PL from delocalized carriers in the wetting layer is observed. In that case nuclear spin polarization initialized by the pump pulse is likely to have a more uniform distribution around the dot.

Symbols in Fig. 4(a) show nuclear spin decay dynamics in a negatively charged dot X^- N4 in the high-density sample. The data were measured in magnetic field $B_z = 8$ T for both σ^+ and σ^- pumping. In this experiment each point has been measured in a single pump-probe cycle. There is no significant decay of nuclear spin polarization at $t_{delay} \lesssim 100$ s. However, for longer delays B_N fluctuates from zero to the level close to the initial polarization B_N^{pump}. Such large fluctuations of B_N with a random telegraph noise character observed after long delays mean that the nuclear spin decay in the QD is controlled by random discrete processes and cannot be described by a continuous function $B_N(t_{delay})$. However, in order to obtain a quantitative estimate for the time scale of this process we use exponential approximation with $\tau_{dec}^{X^-,N4} \approx 250$ s shown with solid lines in Fig. 4(a). Pump-probe measurements performed on this dot in a wide range of B_z reveal similar stochastic character of nuclear spin depolarization, which leads to large uncertainty in the $\tau_{dec}^{X^-,N4}$ estimate.

The dependence of $\tau_{dec}^{X^-,N4}$ on B_z is shown in Fig. 3 with squares. We find that the decay time varies between 10^2 and 10^3 s when B_z changes from 0.3 to 8 T (the uncertainty in τ_{dec} measurements is also connected with the nonexponential decay). Measurements of spin dynamics at zero field allow to estimate only the order of the decay time due to the smallness of B_N that can be pumped under this condition. Nevertheless, a significant decrease in $\tau_{dec}^{X^-,N4}$ down to 1–10 s can be clearly detected and is due to the effect of the dipole-dipole interaction.[31] We also find that variation in the pump time t_{pump} from $2 \times t_{buildup}$ to $50 \times t_{buildup}$ in high magnetic field does not lead to any noticeable change in the nuclear spin decay dynamics, emphasizing that nuclear spin diffusion during the pump pulse is negligible in this negatively charged dot.

We have also studied nuclear spin relaxation processes in dots with differing charge states at high external field $B_z = 4.1$ T when the nuclear-nuclear dipole-dipole interaction is largely suppressed. Figure 4(b) shows decay curves for two positively charged dots X^+ N2 (circles) and X^+ N5 (squares) in the LD sample. In contrast to X^- N4, decay in positively charged dots does not show any fluctuations exceeding experimental error, the symbols and error bars on the graph correspond to an average and standard deviation over several measurements taken for the same delay. Nuclear polarization in dot N2 decays only to ~50% of its initial value for the longest delay time of 4000 s, with exponential fit (dashed line) giving $\tau_{dec}^{X^+,N2} \approx 4200$ s. In dot N5 spin relaxation is significantly faster and is strongly nonexponential (an exponent with $\tau_{dec}^{X^+,N5} = 85$ s is shown with a solid line for comparison). The decay of nuclear polarization in X^+ N5 is very fast at the initial stage with a subsequent slowing down at longer delay times, compared to the relaxation determined by a linear process. Such spin decay is characteristic of nuclear spin diffusion.

Figure 4(c) shows the results of the same experiments repeated for a neutral dot (X^0 N3, circles) and for a negatively charged dot (X^- N1, squares) from the LD sample. Exponential approximations shown with lines yield $\tau_{dec}^{X^0,N3} \approx 350$ s and $\tau_{dec}^{X^-,N1} \approx 5800$ s, respectively. The decay in the neutral dot is more satisfactorily described with a single exponent compared to the decay dependence in the positively charged dot X^+ N5. We also note that in the neutral dot fluctuations of B_N at delays $t_{delay} \sim 300$ s exceed experimental error, although they are not as pronounced as in the negatively charged dot X^- N4 [see Fig. 4(a)].

V. DISCUSSION

In this section we will discuss the nuclear spin dynamics observed in the previous sections with a particular focus on possible mechanisms leading to slow nuclear spin decay. The latter will be discussed in terms of suppression of nuclear spin diffusion. The two possible mechanisms leading to such suppression are the QI and inhomogeneous Knight field of the electron confined in the dot. We will show that both mechanism must be taken into account in order to describe the whole set of data for neutral and charged dots described above.

In indium phosphide ^{31}P nuclei account only for ~8% of the maximum Overhauser shift,[35] which means that large nuclear polarization of ~50% observed in this work is mainly due to ^{115}In spins with $I = 9/2$. Nuclear spin relaxation time of ^{115}In in bulk InP at low temperature was found to be $\tau_{dec} \approx 450$ s in n-type material and was ascribed to hyperfine interaction with conduction electrons[45] while in semi-insulating InP spin-relaxation time of $\tau_{dec} \approx 7000$ s has been reported.[19] We also note that In nuclei have large quadrupolar moment $Q \approx 0.8 \times 10^{-24}$ cm^2 while $Q = 0$ for P nuclei.

Inhomogeneous distribution of nuclear polarization in quantum dots may lead to effective spin relaxation via spin diffusion.[39,46,47] Estimates and experiments show that spin-diffusion coefficients in different semiconductors have similar values of $D \sim 10^{-13}$–10^{-12} cm^2/s.[46,48] Calculation of spin diffusion for QDs with typical dimensions of the studied InP dots with $D \approx 10^{-13}$ cm^2/s yield decay times on the order of

~ 5 s. In all studied InP dots spin decay times exceed $\tau_{dec} \gtrsim 80$ s corresponding to *suppression* of spin diffusion. The longest decay times of strongly inhomogeneous nuclear polarization ($\tau_{dec} \approx 5800$ s, X^- N1) are comparable to the decay time of the uniform spin polarization in bulk material, which means that suppression of spin diffusion can be almost complete. It follows from our experiments that this suppression is dot dependent: nuclear spin decay time is found to vary by ~ 70 times (X^- N1 and X^+ N5) in the same sample.

Furthermore, we find that nuclear polarization measured in X^- N4 after the delay can vary from measurement to measurement [Fig. 4(a)]: B_N can decay almost to zero in less than 200 s, whereas in several instances a substantial nuclear polarization can be detected at delays longer than 1000 s after the pump pulse, implying that strong suppression of spin diffusion similar to the case of X^- N1 can take place. This cannot be a result of statistic fluctuations in the system consisting of $\gtrsim 10^4$ nuclei, which means that spin relaxation in the dot X^- N4 is triggered by discrete processes.

Thus we need to explain the following major tendencies in nuclear polarization decay in dots randomly charged by residual doping: (i) spin-diffusion suppression and (ii) strong dot-to-dot variation in spin relaxation as well as strong fluctuations in the spin decay observed in some dots.

One possible way to suppress spin diffusion is to create a uniform spin distribution by pumping nuclear spin in the material surrounding the dot.[46] However, in the case of high power excitation, leading to nuclear spin pumping via delocalized electrons in the wetting layer, no significant slowing down of spin relaxation was observed ($\tau_{dec}^{X^0,N3} \approx 350$ s in a neutral dot). Much longer decay times are observed in other dots for low power pumping with relatively short optical pulses ($\tau_{dec}^{X^-,N1} \approx 5800$ s in a negatively charged dot). We therefore conclude that an explanation based on the uniform nuclear spin pumping in the material surrounding the dot can be ruled out.

Another mechanism of spin-diffusion suppression involves inhomogeneous shifts of nuclear Zeeman energies due to quadrupolar interaction resulting from electric field gradients. In the simple case when gradients are induced by uniaxial elastic strain along Oz direction parallel to magnetic field the QI Hamiltonian for nuclear spin $I \geq 1/2$ can be written as[48]

$$\hat{H}_Q = h\nu_Q[\hat{I}_z^2 - I(I+1)/3]/2, \tag{2}$$

where ν_Q is a quadrupolar frequency proportional to the component of the deformation tensor $\nu_Q \propto e_{zz}$. The magnitude of QI can also be expressed in terms of effective magnetic field $B_Q = 2\pi\nu_Q/\gamma$. External magnetic field $\vec{B}$ acts on the nuclear spin via the standard Zeeman Hamiltonian

$$\hat{H}_Z = \hbar\gamma(\hat{\vec{I}}, \vec{B}), \tag{3}$$

where γ is a gyromagnetic constant. The quadrupolar fields in InP for a typical deformation $e_{zz} \approx 0.02$ have been estimated[22] to be $B_Q \approx 100$ mT. For a large external field $B_z > B_Q$ QI Hamiltonian (2) gives rise to nonequidistant shifts of the nuclear Zeeman levels. Nonuniform strain distribution also leads to position dependent ν_Q resulting in an energy mismatch between the adjacent nuclei. These two reasons lead to significant reduction in the nuclear flip-flop probability. Such mechanism of diffusion suppression has been shown to result in long spin lifetimes of $\tau_{dec} \sim 3600$ s in InGaAs/GaAs QD structures[21] where strain arises from the lattice mismatch of $\sim 3\%$ between InGaAs and GaAs. The studied InP/GaInP structures have lattice mismatch $\sim 3\%$ (Ref. 49) similar to InGaAs/GaAs and consequently In nuclei that have a large quadrupolar moment are also expected to exhibit strong quadrupole effects. We argue that QI plays a significant role in stabilization of nuclear spin on the dots, as even the fastest decay dynamics observed in this work suggest considerable suppression of spin diffusion.

On the other hand, strong dot-to-dot variation in spin decay times means that either QI is dot dependent or that in some dots an additional relaxation mechanism is possible. Variation in QI in different dots, although possible, seems rather unlikely. From our spectroscopy studies we find that all of the dots have very similar characteristics: magnitude and anisotropy of in-plane hole g factors in charged dots (that is, the same magnitude of heavy-light hole mixing caused by symmetry reduction), dark-bright exciton splitting in neutral dots (anisotropy of e-h exchange interaction caused by lattice mismatch and exciton confinement), diamagnetic shifts and ground-state PL energies (sizes and material compositions of the dots). We thus expect these dots to have similar electric field gradients responsible for QI.

Variation in the spin depolarization times may arise from differing efficiency of interaction with the charges in the dot environment. For example, in negatively charged InGaAs dots embedded in Schottky diode structures, spin decay was found to take place on a millisecond time scale[20] mainly due to the interaction of the charge on the dot with the electron sea in the gate leading to the electron cotunneling.[50] In our gate-free samples the dots may, in principle, still interact with charge reservoirs, which may exist in adjacent fully developed InP dots that can accumulate large numbers of electrons[26] and thus effectively act as an "electron sea." Random behavior in the nuclear spin dynamics observed in X^- N4 can be explained by random, low probability fluctuations of charges in the dot and its environment due to the presence of such electron reservoirs. Strong interactions with neighboring dots are particularly probable in high-density sample. On the other hand, we find fast spin relaxation in positively charged and neutral dots (X^+ N5 and X^0 N3), where the effect of cotunneling is either negligible (due to the small hyperfine coupling and large mass of the hole) or absent (in the neutral dots). Thus explanation based on cotunneling effect requires an assumption that some dots can capture extra electrons in the absence of photoexcitation (see discussion below). At this point we can conclude that explanation of the observed spin dynamics based on the effect of QI is possible, but meets certain difficulties, and may in addition require consideration of other dot-dependent factors such as the interaction with the local charge environment.

An alternative mechanism of the nuclear spin stabilization is the interaction of nuclei with the inhomogeneous Knight field of the confined electron, the effect considered theoretically by Deng and Hu.[23] The electron in the dot with spin $\vec{s}$

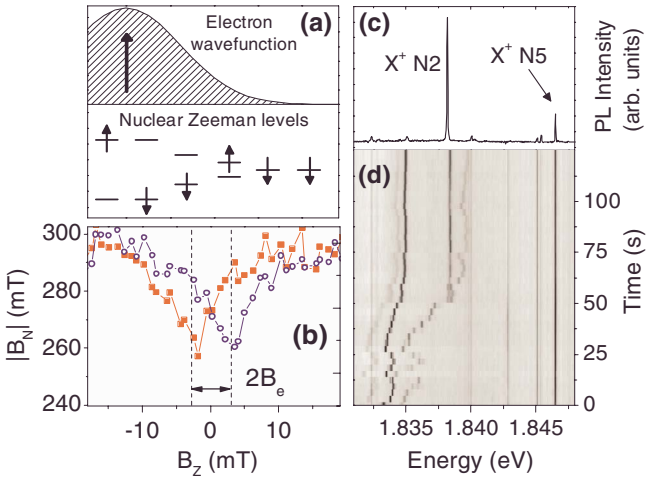

FIG. 5. (Color online) (a) Schematic representation of the effect of a trapped electron on nuclear spin on the dot: inhomogeneous Knight field causes energy splitting mismatch between different nuclei, leading to suppression of nuclear spin diffusion out of the dot. (b) Magnetic field dependence of the nuclear polarization $|B_N|$ on the negatively charged dot N4 under σ^+ (squares) and σ^- (circles) excitations. The observed minima of nuclear polarization correspond to the situation when the external field B_z compensates electron Knight field $\pm B_e$ induced by $\sigma^\pm$ excitation, resulting in partial depolarization of nuclei. The value of $\langle B_e \rangle \approx 3$ mT is estimated from splitting between the minima. [(c) and (d)] PL spectrum from the aperture containing two positively charged dots (X^+ N2 and N5) (c) at a low excitation power 10 μW and (d) its time dependence under high power (200 μW) excitation. Dot N2 and additional spectral features observed at high power demonstrate a large random spectral drift while PL from the dot N5 is stable in time.

acts on the nuclei with the Knight field $\vec{B}_e$ proportional to the envelope wave-function density $|\psi(r)|^2$ at the nucleus site $\vec{r}$,

$$\vec{B}_e(\vec{r}) = \frac{A|\psi(\vec{r})|^2}{\hbar\gamma}\vec{s}, \tag{4}$$

where $A \approx 47(36)$ μeV is a hyperfine interaction constant of indium (phosphorus) in InP.[35] Position-dependent B_e leads to a strong inhomogeneity in the nuclear Zeeman splitting [see diagram in Fig. 5(a)] and, as a consequence, to suppression of nuclear spin diffusion.

The hyperfine field of the electron on the dot can be measured directly from the magnetic field dependence of the Overhauser field $|B_N|$ at low $|B_z| < 20$ mT under circularly polarized excitation[15,51] as shown in Fig. 5(b) for negatively charged dot N4. When an external magnetic field compensates the inhomogeneous Knight field for a portion of the QD nuclear spins, the Zeeman splitting becomes zero for these nuclei. This enhances spin relaxation, observed as a partial decrease (<10%) of the Overhauser field. Excitation with the opposite circular polarization creates a Knight field of the opposite sign. The splitting $2\langle B_e \rangle$ between the minima of $|B_N|$ curves for the two polarizations gives the average Knight field $\langle B_e \rangle \approx 3$ mT. Taking into account the PL polarization degree $\rho_c \approx -30\%$, directly corresponding to the electron-spin polarization, we find that the actual value of the Knight field amounts to $B_e \approx 10$ mT.[52] Assuming a disk-shaped QD with height $z_0 = 4$ nm and diameter $d_0 = 30$ nm we can estimate the mean variation in the Knight field over the distance between adjacent nuclei of the same sort $\approx 0.7 \times l_0$ ($l_0 \approx 0.5$ nm is a unit-cell size) to be $\Delta B_e^z \approx 1.8$ mT and $\Delta B_e^{x,y} \approx 0.25$ mT in directions normal and parallel to the sample surface, respectively.

The estimated differences of nuclear spin splitting between neighboring nuclei exceed the nuclear spin level broadening, which is expected to be on the order of the local field $B_L \sim 0.1$ mT (Ref. 31) created by the nuclear dipole-dipole interaction.[53] Such Zeeman splitting mismatch between adjacent nuclei reduces the probability of nuclear spin transfer via the flip-flops suppressing spin diffusion out of the dot. Importantly, the effect of the Knight field is more pronounced for Oz direction normal to the larger top/bottom surface of the dot, while spin diffusion through the smaller side surface of the dot, where Knight-field gradient is smaller, is less significant due to the small height to width ratio of the studied dots (estimated to be less than 1/10). This rough estimate is confirmed by more comprehensive analysis in Ref. 23. Thus, due to the reduced spin leakage into the surrounding bulk in a negatively charged dot (as in X^- N1), electron and nuclei can form a closed system with the stable total spin. By contrast, hole confined on the dot will not lead to nuclear spin freezing due to weak hyperfine interaction for p-type wave functions ($\sim$10% of that for s-type states[54]).

This suppression mechanism allows to explain relatively fast relaxation in positively charged and neutral dots (X^+ N5 and X^0 N3), where spin diffusion is reduced only due to QI (in the neutral dot diffusion might be also suppressed due to more uniform initial polarization caused by the higher power of the pump, see Sec. IV B). Taking into account possible charge instabilities in the dot environment, it is also possible to explain the random behavior of the nuclear spin decay in X^- N4: if the electron hops out of the dot during the dark time, the stabilizing Knight field disappears enabling the nuclear spin relaxation due to the dipole-dipole interaction, leading, in particular, to nuclear spin diffusion. However, slow spin dynamics observed in the positively charged dot X^+ N2 still conflict with this model.

As in the case of QI-induced stabilization, this discrepancy can be resolved if we consider the possibility of the dot recharging, when the laser excitation is completely blocked during the pump-probe delay, similar to the assumed random jumps of the electron responsible for large fluctuations of spin polarization in X^- N4. In fact, this particular dot (X^+ N2) is found to be more prone to the random recharging than the other dots studied. Figure 5 shows PL spectrum of the 800 nm aperture with both positively charged dots X^+ N2 and N5 at low excitation $P_{exc} \approx 10$ μW (c) and temporal dependence of the spectrum at increased power $P_{exc} \approx 200$ μW (d). It can be seen that at high excitation power PL of the dot N2 can completely disappear from the spectrum, this process is accompanied by a large spectral drift of additional spectral features. At the same time PL from the dot N5 is very stable–its spectral position remained unchanged for >1000 h of experimental studies.

As mentioned above, the absence of the electric gate is essential in eliminating fast spin relaxation via cotunneling

but it brings the disadvantage of uncertainty in the charge state of the dot and insufficient control of its electrostatic environment. Even low power photoexcitation may change charge distribution in the neighboring dots and wetting layer. Thus, for some dots the charge state in the dark condition may differ from that observed in photoluminescence. The explanation of the long spin lifetime in X^+ N2 within the Knight-field stabilization concept requires the assumption that this dot, observed as a positively charged in PL, changes its state to negatively charged once photoexcitation has been switched off. Such recharging can take place if the dot reversibly captures two additional electrons when it is not illuminated. Verification of the discussed role of the electron on the nuclear spin dynamics requires further studies using QD structures with electrically controlled charging but with small tunneling rate into the contact.

VI. CONCLUSION

In conclusion, experimental studies of optically induced nuclear spin dynamics in charged InP/GaInP quantum dots in electric-contacts-free structures revealed long-lived nuclear polarization in singly negatively and positively charged as well as in neutral dots. The spin depolarization decay time in the dark varies from ~85 to ~6000 s, the latter observed for a negatively charged dot and corresponding to almost complete suppression of nuclear spin diffusion out of the dot. This is in strong contrast to previous observations of nuclear spin depolarization on the millisecond time scale in negatively charged dots in Schottky devices, explained by the electron cotunneling to the contacts. To explain the observed suppression of nuclear spin diffusion, we have examined two recently proposed mechanisms, including quadrupole effects and stabilization arising from the inhomogeneous Knight field of the electron confined on the dot. It is shown that both concepts can only partly explain the experimental observations and require additional relaxation mechanism to account for strong variation in nuclear spin dynamics in different dots. We argue that the charge dynamics in the dot and its environment due to residual doping and photoexcitation can have a strong effect on nuclear spin dynamics. The lack of precise control over the dot charge state hinders controlled manipulation of the nuclear spin dynamics on the dot, which will be resolved in further studies on doped samples or carefully designed charge-tunable devices.

ACKNOWLEDGMENTS

We thank A. J. Ramsay and V. Fal'ko for fruitful discussions. This work was supported by the EPSRC under Grants No. EP/C54563X/1, No. EP/C545648/1, No. GR/S76076, and No. EP/G601642/1, and by the Royal Society.

APPENDIX: PHOTOLUMINESCENCE OF InP/GaInP QUANTUM DOTS WITH DIFFERENT CHARGE STATES

Figure 6(a) shows PL spectra of a single quantum dot N3 from LD sample measured in circular polarizations of detection in Faraday geometry ($B \| Oz$) and in two orthogonal linear polarizations in Voigt geometry ($B \| Ox$). Energies of all

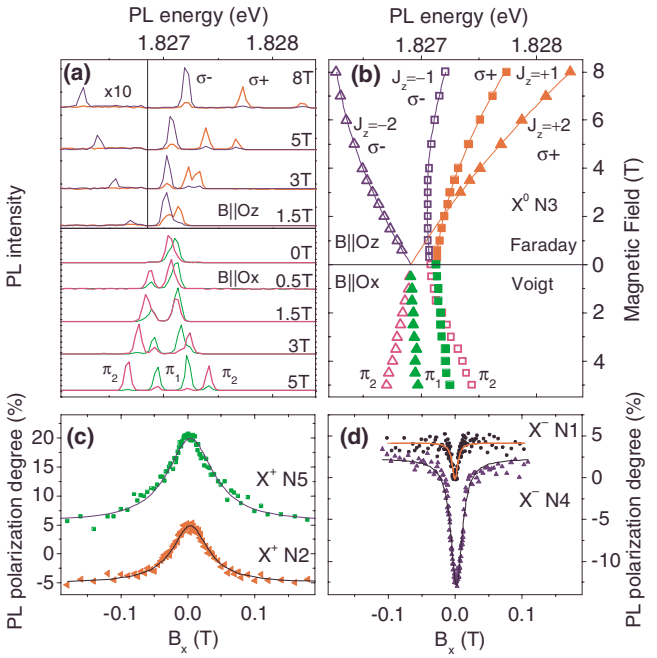

FIG. 6. (Color online) (a) Photoluminescence spectra of a neutral exciton X^0 (dot N3) measured in σ^+ and σ^- circular polarizations in Faraday ($B \| Oz$) geometry (σ^--polarized excitation) and in orthogonal π_1, π_2 linear polarizations in Voigt ($B \perp Oz$) geometry (linearly polarized excitation). Low energy parts of the spectra in Faraday geometry separated by vertical line are multiplied by 10. (b) Energies of PL lines deduced from spectra in panel (a) as a function of magnetic field. Exciton components originating from bright $J_z = \pm 1$ (dark $J_z = \pm 2$) states are shown with squares (triangles). Solid lines show approximation (see explanation in text). [(c) and (d)] Hanle effect measurements for various charged dots. Circular polarization degree of PL under circularly polarized excitation is shown as a function of in-plane magnetic field B_x for (c) positively and (d) negatively charged dots. Solid lines show best fit with Lorenz function. The products of depolarization times and g factors are found from the fitting: $gT = 350$ ps (X^+ N2, LD sample), 280 ps (X^+ N5, LD sample), 2.3 ns (X^- N1, LD sample), and 1.1 ns (X^- N4, HD sample).

PL lines resolved in this experiment are shown as a function of magnetic field in Fig. 6(b). Linearly polarized doublet at zero magnetic field with spectral splitting $\delta_b \approx 60$ μeV is characteristic of an exciton (X^0) luminescence in a neutral dot.[55] This is further confirmed by observation of a biexciton (XX^0) doublet with equal splitting and reversed order of linearly polarized components ~5 meV below exciton emission[29] at high excitation density [not shown in Fig. 6(a)]. Magnetic field parallel to the sample surface mixes the states of the optically active (bright) doublet with moment projection $J_z = \pm 1$ and dark exciton states with $J_z = \pm 2$.[55] As a result, the latter gain nonzero oscillator strength, which is observed as an additional line emerging ~0.2 meV bellow the allowed doublet at a relatively small magnetic field $B_x = 0.5$ T. High magnetic field parallel to the sample surface splits both bright and dark states into four well-resolved linearly polarized components.

Magnetic field normal to the sample surface increases the splitting of the bright doublet converting linear polarizations

into circular. In this particular dot it also enables weak emission of the dark exciton. This can be a result of reduced quantum dot shape symmetry or due to the slight tilt of the dot quantization axis. PL intensity of high-energy dark line with $J_z=+2$ is considerably increased at $B_z \sim 2.5$ T, signifying anticrossing with $J_z=+1$ state due to electron-hole exchange interaction.[55–57] PL intensity of the $J_z=\pm 2$ states saturates at much smaller excitation power than for the $J_z=\pm 1$ states. The maximum intensity of the $J_z=-2$ component, which is well separated from all other lines, is only ~ 0.01 of the maximum intensity of $J_z=\pm 1$ states at $B_z=8$ T. This gives an estimate of the mixing between bright and dark exciton states induced by magnetic field $B \| Oz$.

Observation of the dark states in Faraday geometry makes it possible to deduce the g factors of electrons and holes independently from a single measurement. Due to smallness of dark-bright mixing magnetic field dependence of exciton PL energies can be described using the well-known expressions:[55] $E_b(B_z)=E_0+\kappa B_z^2+\delta_0/2 \pm \sqrt{\delta_b^2+\mu_B^2(g_{h,z}-g_{e,z})^2B_z^2}/2$ for bright $J_z=\pm 1$ states and $E_d(B_z)=E_0+\kappa B_z^2-\delta_0/2 \pm \sqrt{\delta_d^2+\mu_B^2(g_{h,z}+g_{e,z})^2B_z^2}/2$ for dark $J_z=\pm 2$ states. In these equations E_0 and μ_B stand for quantum dot band-gap energy and Bohr magneton, respectively. From the approximation shown by solid lines in Fig. 6(b) we find diamagnetic shift $\kappa \approx 5.8$ μeV/T^2, dark-bright splitting $\delta_0 \approx 200$ μeV, and bright exciton doublet splitting $\delta_b \approx 65$ μeV, dark exciton splitting δ_d cannot be resolved and was kept zero in approximation. Using the order of σ^+- and σ^--polarized components at high magnetic field electron and hole g factors are found to be $g_{e,z} \approx +1.6$ and $g_{h,z} \approx +2.7$. We note that exciton-biexciton splitting and dark-bright splitting δ_0 have very close values in all neutral dots while the fine-structure splitting δ_b as well as the presence of the dark components induced by $B \| Oz$ vary strongly from dot to dot.

In contrast to neutral dots PL of singly charged dots at zero magnetic field consists of a single unpolarized line that splits into four linearly polarized components of similar intensities in magnetic field parallel to the surface.[55] A detailed characterization of negatively charged dots in these structures can be found in Ref. 24, where electron (hole) g factors were found to be $g_{e,z}(g_{h,z}) \approx +1.5(+2.8)$, in good agreement with neutral dots. Fine structure of positively and negatively charged dots is very similar. We use Hanle effect measurements to establish the sign of the charge in each particular dot.[58] PL circular polarization degree defined as $\rho_c=(I_{co}-I_{cross})/(I_{co}+I_{cross})$, where I_{co} (I_{cross}) is the intensity of luminescence co(cross)polarized with exciting circularly polarized laser, has been measured as a function of in-plane magnetic field B_x. Polarization of the excitation has been switched between σ^+ and σ^- using a Pockels cell at a frequency of 16 kHz in order to suppress nuclear spin polarization. Figures 6(c) and 6(d) show depolarization curves of two clearly different types measured on charged dots. For the curves shown in Fig. 6(c) we find suppression of positive polarization, Lorenz fits shown with solid lines give Hanle widths of $B_0 \approx 35$ mT. On the other hand, two dots in Fig. 6(d) demonstrate suppression of negative circular polarization[59,60] by in-plane magnetic field B_x, the smallest depolarization curve width is $B_0 \approx 5$ mT. Using electron g factor we find depolarization times for the dots shown in Fig. 6(d) to be 1.5 ns (dot N1, LD sample) and 0.8 ns (dot N4, HD sample). The value for the dot N1 exceeds recombination lifetime ≈ 1 ns measured in this structures, which allows us to attribute these curves to spin lifetime of the residual electron in negatively charged (X^-) dots.[58,61] We ascribe the curves in Fig. 6(c) to depolarization of the photoexcited electron of the positively charged trion. The spin depolarization times are found to be 230 and 190 ps for X^+ of dot N2 and of dot N5, respectively (both dots are from LD sample). Faster depolarization in case of positively charged dots compared to X^- is a result of the combined effect of spin relaxation and radiative decay of the X^+ trion.

*Present address: Toshiba Research Europe Ltd., 208 Cambridge Science Park, Cambridge CB4 0GZ, UK.

[1] D. Loss and D. P. DiVincenzo, Phys. Rev. A **57**, 120 (1998).
[2] A. E. Dementyev, D. G. Cory, and C. Ramanathan, Phys. Rev. Lett. **100**, 127601 (2008).
[3] H. Hayashi, K. M. Itoh, and L. S. Vlasenko, Phys. Rev. B **78**, 153201 (2008).
[4] D. K. Wilson and G. Feher, Phys. Rev. **124**, 1068 (1961).
[5] B. E. Kane, Nature (London) **393**, 133 (1998).
[6] G. W. Morley, J. van Tol, A. Ardavan, K. Porfyrakis, J. Zhang, and G. A. D. Briggs, Phys. Rev. Lett. **98**, 220501 (2007).
[7] M. V. G. Dutt, L. Childress, L. Jiang, E. Togan, J. Maze, F. Jelezko, A. S. Zibrov, P. R. Hemmer, and M. D. Lukin, Science **316**, 1312 (2007).
[8] L. Childress, M. V. Gurudev Dutt, J. M. Taylor, A. S. Zibrov, F. Jelezko, J. Wrachtrup, P. R. Hemmer, and M. D. Lukin, Science **314**, 281 (2006).
[9] R. Hanson, V. V. Dobrovitski, A. E. Feiguin, O. Gywat, and D. D. Awschalom, Science **320**, 352 (2008).
[10] F. H. L. Koppens, C. Buizert, K. J. Tielrooij, I. T. Vink, K. C. Nowack, T. Meunier, L. P. Kouwenhoven, and L. M. K. Vandersypen, Nature (London) **442**, 766 (2006).
[11] J. R. Petta, A. C. Johnson, J. M. Taylor, E. A. Laird, A. Yacoby, M. D. Lukin, C. M. Marcus, M. P. Hanson, and A. C. Gossard, Science **309**, 2180 (2005).
[12] A. Imamoğlu, E. Knill, L. Tian, and P. Zoller, Phys. Rev. Lett. **91**, 017402 (2003).
[13] D. J. Reilly, J. M. Taylor, J. R. Petta, C. M. Marcus, M. P. Hanson, and A. C. Gossard, Science **321**, 817 (2008).
[14] D. Gammon, S. W. Brown, E. S. Snow, T. A. Kennedy, D. S. Katzer, and D. Park, Science **277**, 85 (1997).
[15] C. W. Lai, P. Maletinsky, A. Badolato, and A. Imamoglu, Phys. Rev. Lett. **96**, 167403 (2006).
[16] B. Eble, O. Krebs, A. Lemaitre, K. Kowalik, A. Kudelski, P. Voisin, B. Urbaszek, X. Marie, and T. Amand, Phys. Rev. B **74**, 081306(R) (2006).
[17] A. I. Tartakovskii, T. Wright, A. Russell, V. I. Fal'ko, A. B. Van'kov, J. Skiba-Szymanska, I. Drouzas, R. S. Kolodka, M. S. Skolnick, P. W. Fry, A. Tahraoui, H.-Y. Liu, and M. Hopkinson, Phys. Rev. Lett. **98**, 026806 (2007).
[18] M. N. Makhonin, A. I. Tartakovskii, A. Ebbens, M. S. Skolnick, A. Russell, V. I. Fal'ko, and M. Hopkinson, Appl. Phys. Lett.

93, 073113 (2008).
[19] C. A. Michal and R. Tycko, Phys. Rev. Lett. **81**, 3988 (1998).
[20] P. Maletinsky, A. Badolato, and A. Imamoglu, Phys. Rev. Lett. **99**, 056804 (2007).
[21] P. Maletinsky, M. Kroner, and A. Imamoglu, Nat. Phys. **5**, 407 (2009).
[22] R. I. Dzhioev and V. L. Korenev, Phys. Rev. Lett. **99**, 037401 (2007).
[23] C. Deng and X. Hu, Phys. Rev. B **72**, 165333 (2005).
[24] J. Skiba-Szymanska, E. A. Chekhovich, A. E. Nikolaenko, A. I. Tartakovskii, M. N. Makhonin, I. Drouzas, M. S. Skolnick, and A. B. Krysa, Phys. Rev. B **77**, 165338 (2008).
[25] M. Sopanen, H. Lipsanen, and J. Ahopelto, Appl. Phys. Lett. **67**, 3768 (1995).
[26] D. Hessman, J. Persson, M.-E. Pistol, C. Pryor, and L. Samuelson, Phys. Rev. B **64**, 233308 (2001).
[27] M.-E. Pistol, J. Phys.: Condens. Matter **16**, S3737 (2004).
[28] E. A. Chekhovich, M. N. Makhonin, K. V. Kavokin, A. B. Krysa, M. S. Skolnick, and A. I. Tartakovskii, Phys. Rev. Lett. **104**, 066804 (2010).
[29] G. J. Beirne, M. Reischle, R. Roßbach, W.-M. Schulz, M. Jetter, J. Seebeck, P. Gartner, C. Gies, F. Jahnke, and P. Michler, Phys. Rev. B **75**, 195302 (2007).
[30] A. Hartmann, Y. Ducommun, E. Kapon, U. Hohenester, and E. Molinari, Phys. Rev. Lett. **84**, 5648 (2000).
[31] *Optical Orientation*, edited by F. Meier and B. P. Zakharchenya (Elsevier, New York, 1984).
[32] A. W. Overhauser, Phys. Rev. **92**, 411 (1953).
[33] D. Gammon, A. L. Efros, T. A. Kennedy, M. Rosen, D. S. Katzer, D. Park, S. W. Brown, V. L. Korenev, and I. A. Merkulov, Phys. Rev. Lett. **86**, 5176 (2001).
[34] Here we neglect hyperfine coupling of the heavy-hole spin as it is ~10 times smaller (Ref. 54) than for the electron and thus leads only to minor correction of the measured B_N value.
[35] B. Gotschy, G. Denninger, H. Obloh, W. Wilkening, and J. Schnieder, Solid State Commun. **71**, 629 (1989).
[36] B. Urbaszek, P.-F. Braun, T. Amand, O. Krebs, T. Belhadj, A. Lemaitre, P. Voisin, and X. Marie, Phys. Rev. B **76**, 201301(R) (2007).
[37] M. N. Makhonin, J. Skiba-Szymanska, M. S. Skolnick, H.-Y. Liu, M. Hopkinson, and A. I. Tartakovskii, Phys. Rev. B **79**, 125318 (2009).
[38] We note that under σ^--polarized excitation residual electrons in negatively charged dots and photoexcited electrons in positively charged dots have spin polarization of the same sign resulting in positive nuclear field ($B_N>0$) in both cases. This is due to negative circular polarization ($\rho_c<0$) observed in negatively charged dots while $\rho_c>0$ is found for positively charged dots (see Fig. 6). In the opposite case studied by Lai *et al.* (Ref. 15) $\rho_c>0$ for both signs of the dot charging and the resulting B_N has opposite signs in positively and negatively charged dots.
[39] A. E. Nikolaenko, E. A. Chekhovich, M. N. Makhonin, I. W. Drouzas, A. B. Van'kov, J. Skiba-Szymanska, M. S. Skolnick, P. Senellart, D. Martrou, A. Lemaître, and A. I. Tartakovskii, Phys. Rev. B **79**, 081303(R) (2009).
[40] V. L. Korenev, JETP Lett. **70**, 129 (1999).
[41] D. Paget, T. Amand, and J.-P. Korb, Phys. Rev. B **77**, 245201 (2008).
[42] A. Russell, V. I. Fal'ko, A. I. Tartakovskii, and M. S. Skolnick, Phys. Rev. B **76**, 195310 (2007).
[43] P.-F. Braun, B. Urbaszek, T. Amand, X. Marie, O. Krebs, B. Eble, A. Lemaitre, and P. Voisin, Phys. Rev. B **74**, 245306 (2006).
[44] P. Maletinsky, C. W. Lai, A. Badolato, and A. Imamoglu, Phys. Rev. B **75**, 035409 (2007).
[45] B. Clerjaud, F. Gendron, H. Obloh, J. Schneider, and W. Wilkening, Phys. Rev. B **40**, 2042 (1989).
[46] D. Paget, Phys. Rev. B **25**, 4444 (1982).
[47] M. N. Makhonin, A. I. Tartakovskii, A. B. Van'kov, I. Drouzas, T. Wright, J. Skiba-Szymanska, A. Russell, V. I. Fal'ko, M. S. Skolnick, H.-Y. Liu, and M. Hopkinson, Phys. Rev. B **77**, 125307 (2008).
[48] A. Abragam, *The Principles of Nuclear Magnetism* (Oxford University Press, London, 1961).
[49] A. Onton, M. R. Lorenz, and W. Reuter, J. Appl. Phys. **42**, 3420 (1971).
[50] J. M. Smith, P. A. Dalgarno, R. J. Warburton, A. O. Govorov, K. Karrai, B. D. Gerardot, and P. M. Petroff, Phys. Rev. Lett. **94**, 197402 (2005).
[51] R. V. Cherbunin, S. Y. Verbin, T. Auer, D. R. Yakovlev, D. Reuter, A. D. Wieck, I. Y. Gerlovin, I. V. Ignatiev, D. V. Vishnevsky, and M. Bayer, Phys. Rev. B **80**, 035326 (2009).
[52] Measurements performed on different singly charged dots reveal very similar electron Knight fields $B_e \sim 10$ mT. In case of positively charged dots B_e corresponds to the effect of the photoexcited electron of the trion while in negatively charged dots Knight field is induced by the residual charge.
[53] The effect of the electron field on nuclei is significant only if electron-spin lifetime T_1^e exceeds the precession period of the nuclear spin $1/\nu_L$, determined by Larmor frequency which is $\nu_L \approx 9(17)$ MHz/T for indium (phosphorus). The exact value of T_1^e in InP dots at different fields is not available. It is known however that for large enough magnetic field T_1^e can be on a millisecond time scale (Ref. 62). We thus assume that $T_1^e \gg 1/\nu_L$ for $B_z \gtrsim 0.5$ T and the effective field experienced by nuclei equals to the instant value of B_e.
[54] C. Testelin, F. Bernardot, B. Eble, and M. Chamarro, Phys. Rev. B **79**, 195440 (2009).
[55] M. Bayer, G. Ortner, O. Stern, A. Kuther, A. A. Gorbunov, A. Forchel, P. Hawrylak, S. Fafard, K. Hinzer, T. L. Reinecke, S. N. Walck, J. P. Reithmaier, F. Klopf, and F. Schäfer, Phys. Rev. B **65**, 195315 (2002).
[56] L. Besombes, Y. Léger, L. Maingault, D. Ferrand, H. Mariette, and J. Cibert, Phys. Rev. Lett. **93**, 207403 (2004).
[57] Y. Masumoto, K. Toshiyuki, T. Suzuki, and M. Ikezawa, Phys. Rev. B **77**, 115331 (2008).
[58] A. S. Bracker, E. A. Stinaff, D. Gammon, M. E. Ware, J. G. Tischler, A. Shabaev, A. L. Efros, D. Park, D. Gershoni, V. L. Korenev, and I. A. Merkulov, Phys. Rev. Lett. **94**, 047402 (2005).
[59] S. Cortez, O. Krebs, S. Laurent, M. Senes, X. Marie, P. Voisin, R. Ferreira, G. Bastard, J.-M. Gérard, and T. Amand, Phys. Rev. Lett. **89**, 207401 (2002).
[60] S. Laurent, M. Senes, O. Krebs, V. K. Kalevich, B. Urbaszek, X. Marie, T. Amand, and P. Voisin, Phys. Rev. B **73**, 235302 (2006).
[61] Y. Masumoto, S. Oguchi, B. Pal, and M. Ikezawa, Phys. Rev. B **74**, 205332 (2006).
[62] M. Kroutvar, Y. Ducommun, D. Heiss, M. Bichler, D. Schuh, G. Abstreiter, and J. J. Finley, Nature (London) **432**, 81 (2004).